Supplementary Information

A Nickel Phosphine Complex as a Fast and Efficient Hydrogen Production Catalyst

*Lu Gan[†], Thomas L. Groy[†], Pilarisetty Tarakeshwar[†], Shobeir K. S. Mazinani[†], Jason Shearer[§], Vladimiro Mujica[†], Anne K. Jones[†]**

[†]Department of Chemistry and Biochemistry, Arizona State University, Tempe, AZ 85287, USA

[§]Department of Chemistry, University of Nevada, Reno, Nevada 89557, USA

e-mail: jonesak@asu.edu; Tel: 480-965-0356; Fax: 480-965-2747

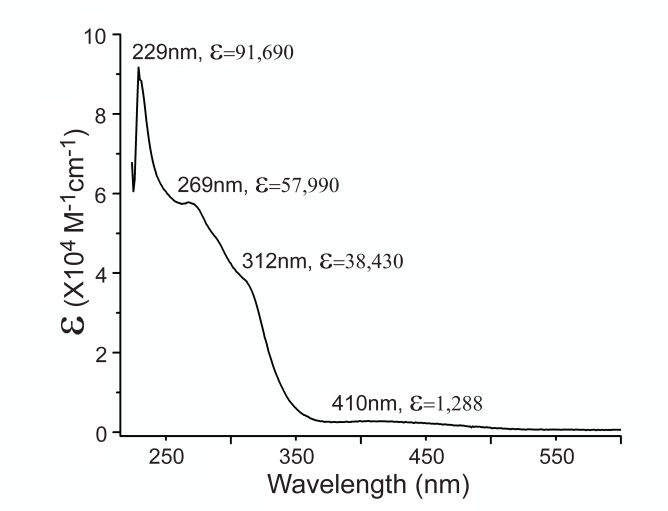

Figure S1. UV-vis absorbance spectrum from a 0.01 mM solution of **1** in dichloromethane.

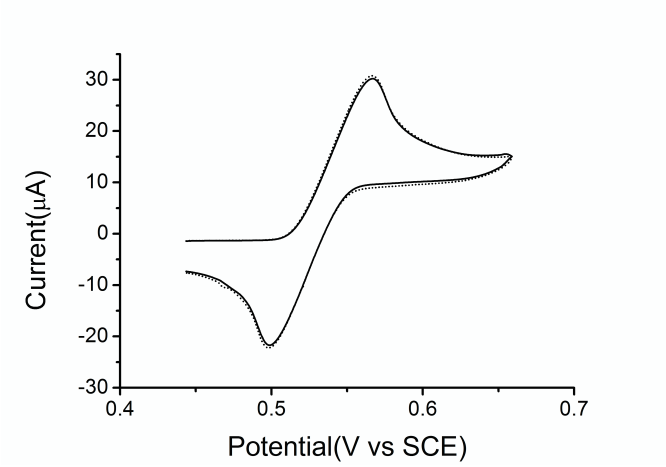

Figure S2. Cyclic voltammograms from ferrocene in THF with 0.1 M $TBAPF_6$ as supporting electrolyte at a potential scan rate of 100 mV s^{-1}. The solid line was recorded in an atmosphere of argon, and the dotted line under an atmosphere of hydrogen.

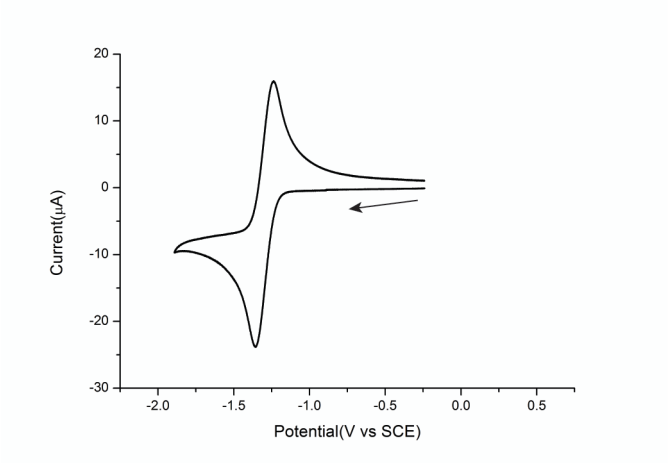

Figure S3. Cyclic voltammogram of **1** featuring only the Ni^{I}/Ni^{II} couple by restricting the range of potentials to -0.2 V to -1.9 V. The arrow marks the starting point and direction of potential cycling. The supporting electrolyte is 0.3 M $TBAPF_6$ in THF, and the potential scan rate is 100 mV s^{-1}.

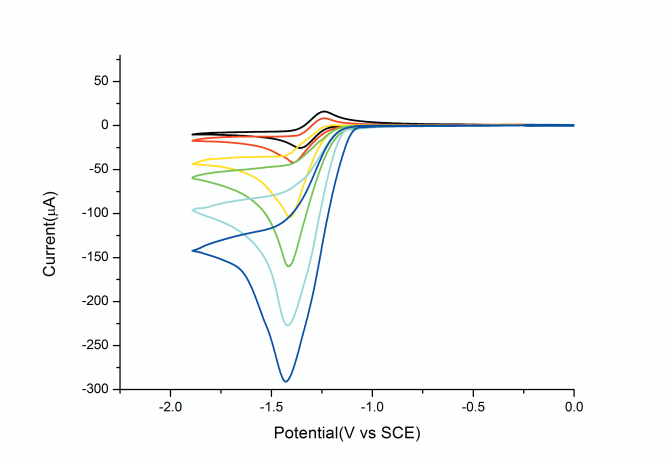

Figure S4. Cyclic voltammograms of 2.5 mM **1** in THF with 0.3 M $TBAPF_6$ as supporting electrolyte in the presence of varying concentrations of *p*-toluenesulfonic acid (pTsOH) under nitrogen at an electrochemical potentials scan rate of 100 mV s^{-1}. The concentrations of pTsOH are 0, 2, 4, 6, 8, and 10 mM.

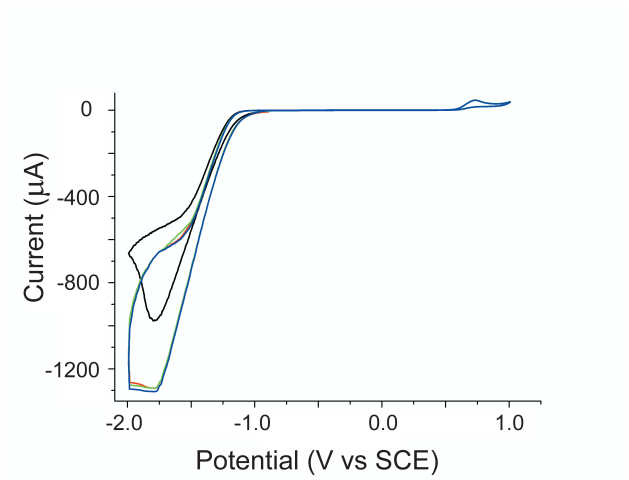

Figure S5. Cyclic voltammograms of **1** with high concentrations of acetic acid, i.e. in the region in which i_c/i_p is independent of acid concentration. Black, 50 equivalents (relative to catalyst). Red, 125 equivalents. Green, 175 equivalents. Blue, 200 equivalents. The supporting electrolyte is 0.3 M $TBAPF_6$ in THF, and the potential scan rate is 100 mV s^{-1}.

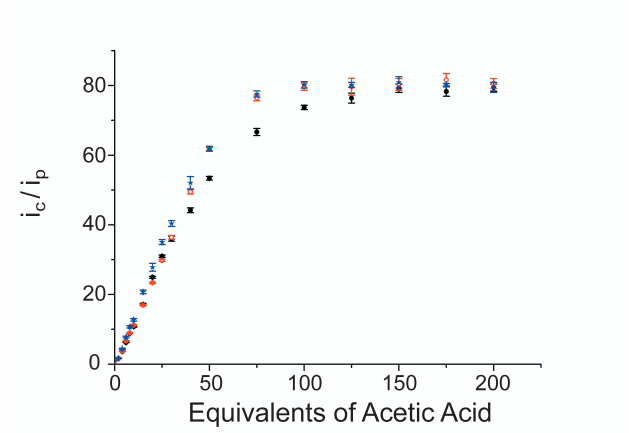

Figure S6. Dependence of normalized catalytic current, i_c, on acetic acid concentration for three difference concentrations of catalyst. Experiments were undertaken at three different catalyst concentrations: black dots, 1 mM catalyst; red dot, 2 mM catalyst; blue star, 3 mM catalyst. The supporting electrolyte is 0.3 M $TBAPF_6$ in THF, and the potential scan rate is 100 mV s^{-1}. Error bars represent one standard deviation from three independent measurements.

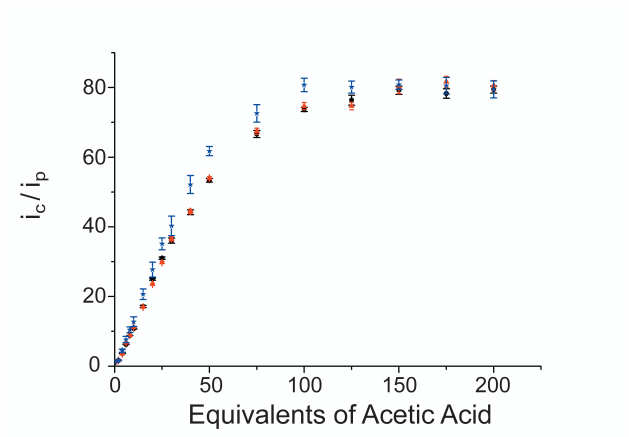

Figure S7. Dependence of normalized catalytic current, i_c, on acetic acid concentration extracted from voltammograms obtained at three different potential scan rates: 10 mV s^{-1} (red triangle), 100 mV s^{-1} (black dot), and 5 V s^{-1} (blue star). Other experimental conditions were 1.0 mM **1** in THF, 0.3 M $TBAPF_6$. Error bars indicate one standard deviation determined from three independent experiments.

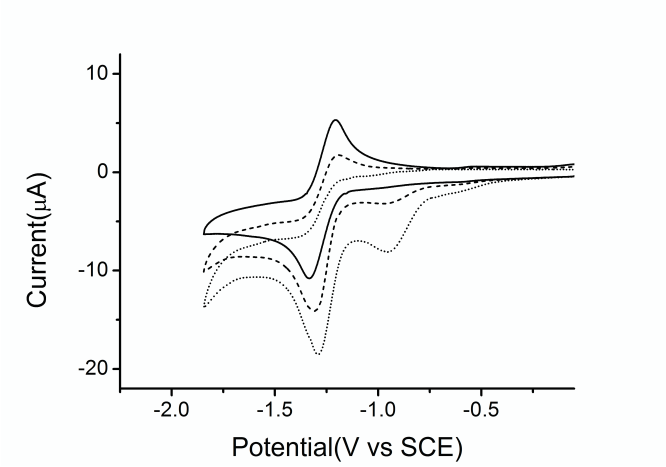

Figures S8. Cyclic voltammograms of **1** in the presence and absence of CO. The solid line shows a voltammogram in an argon saturated solution. The dotted line shows a voltammogram obtained in a solution saturated with CO. The dashed lines shows a voltammogram obtained using a solution that was previously saturated with CO following sparging of the experimental solution with argon. The experimental conditions are 1.1 mM of complex **1**, 0.1 M $TBAPF_6$ in THF and a potential scan rate of 100 mV s^{-1}.

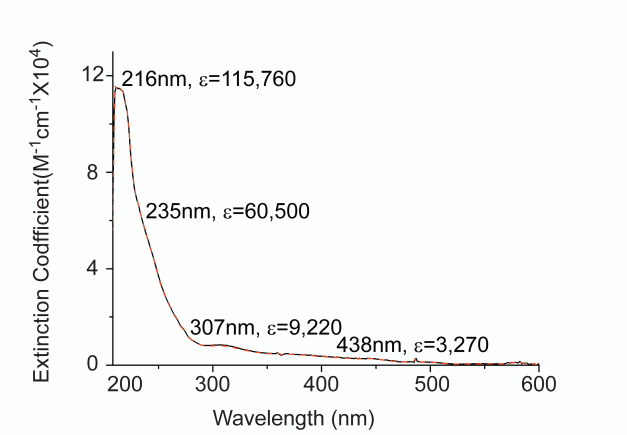

Figure S9. UV-vis absorbance spectrum from a $6.5x10^{-3}$ mM solution of **1** in THF (black) and following exposure to $5x10^{-1}$ mM acetic acid for four hours (red).

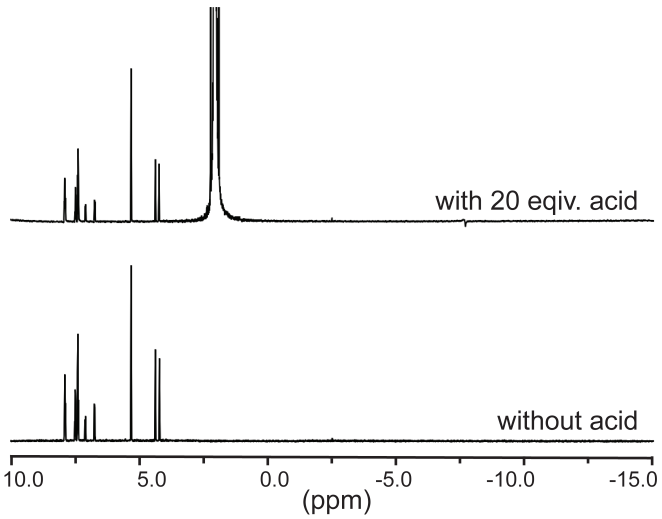

Figure S10. ^{1}H NMR spectrum of **1** in the presence of 20 equivalents of acetic acid in CD_2Cl_2.

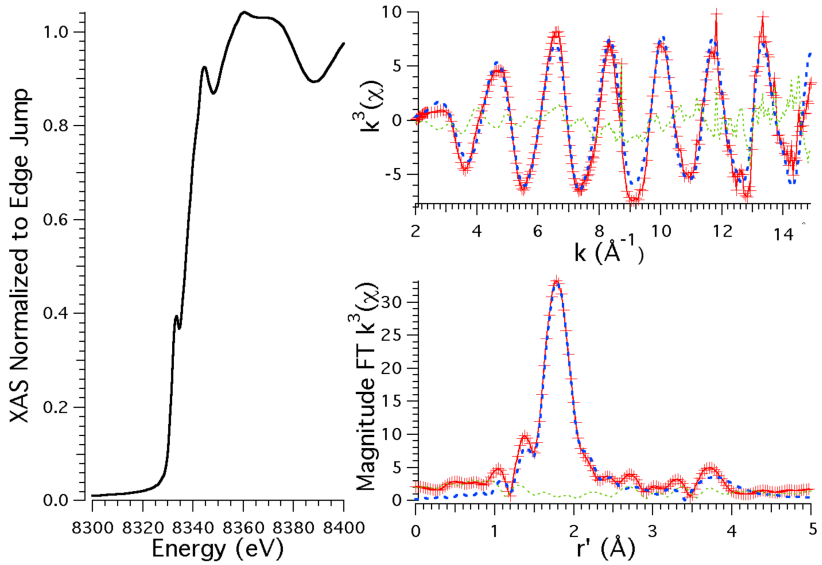

Figure S11. Left: XANES region of the Ni K-edge X-ray absorption spectrum of **1**. Top right: k^3 weighted EXAFS spectrum **1** displaying the data (red line with markers), simulation to the data (dashed blue line) and difference spectrum (dotted green line). Bottom right: Magnitude Fourier Transformed k^3 EXAFS spectrum **1** displaying the data (red line with markers), simulation to the data (dashed blue line) and difference spectrum (dotted green line). Pre-edge peak #1: 8332.7(1) eV (area = 0.02(1) eV relative to the edge); Pre-edge peak #2: 8336.4(1) eV (area = 0.47(1) eV relative to the edge); E_o = 8343.2 eV; Shell #1, Ni-S: n = 2, r = 2.162(2) Å, σ^2 = 0.004(2) Å^2; Shell #2, Ni-P: n = 2, r = 2.271(3) Å, σ^2 = 0.0038(1) Å^2; Shell #3, Ni-Fe: n = 1, r = 4.17(13) Å, σ^2 = 0.001(1) Å^2; ε^2 = 0.10.

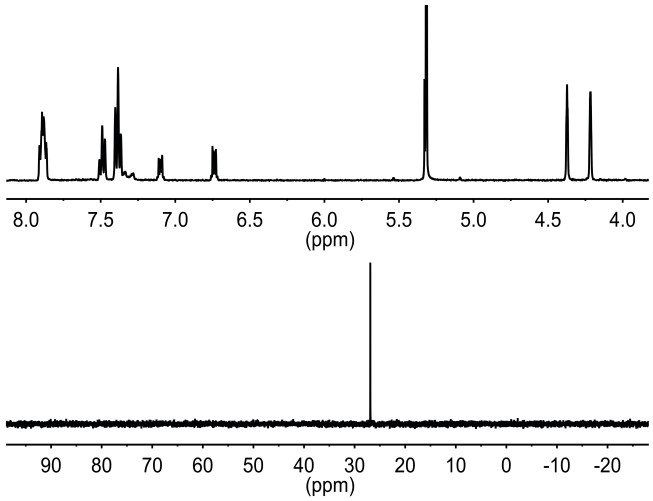

Figure S12. ^{1}H (top) and ^{31}P (bottom) NMR spectrum of **1** in CD_2Cl_2.

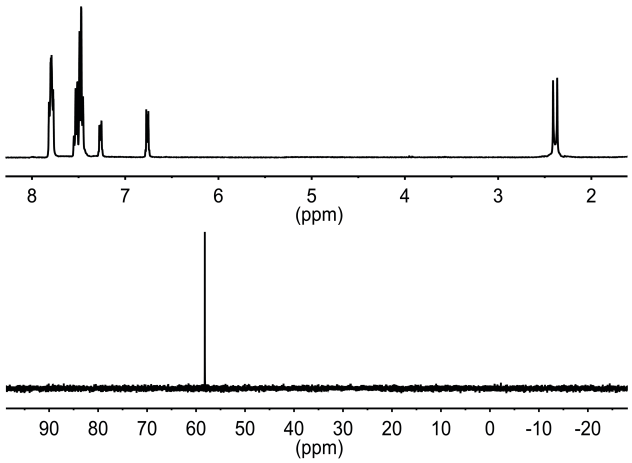

Figure S13. ^{1}H (top) and ^{31}P (bottom) NMR spectrum of **2** in $CDCl_3$.

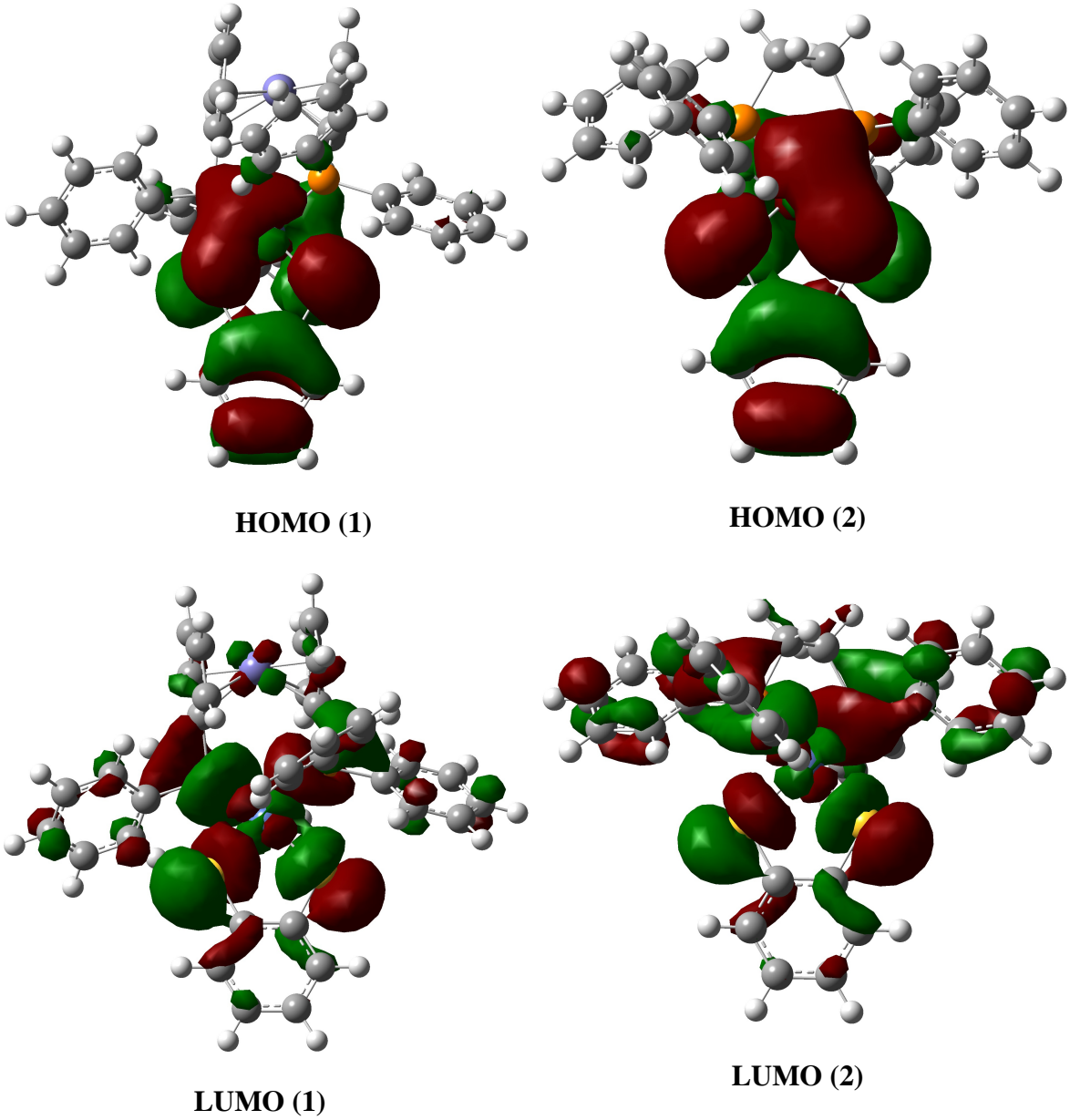

Figure S14. Electron density profiles of the highest occupied molecular orbital (HOMO) and lowest unoccupied molecular orbital (LUMO) of complexes **1**, and **2**, respectively.

*Determination of the ratio of the equilibrium constants for binding hydrogen to the oxidized and reduced forms of **1***

The shift in reduction potential of **1** observed in the presence of hydrogen indicates that hydrogen binds more tightly to the reduced than the oxidized form of the complex. The electrochemical results can be explained by the square scheme below with the thermodynamic parameters defined in the ordinary way.

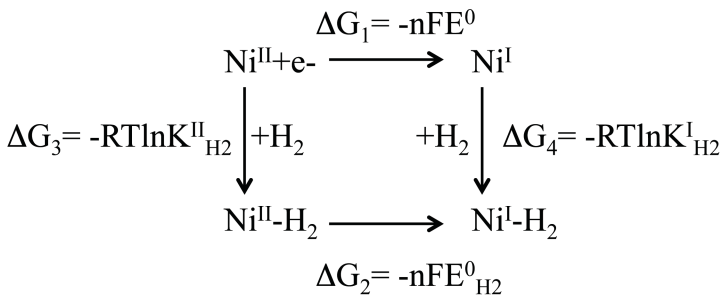

Since the two reduction potentials, E^0 = -1.280 V and $E^0_{H_2}$ = -1.009 V, are determined in the electrochemical experiments, the ratio of the two binding constants can be determined using the following equation derived from Hess's law.

$$\frac{K^{II}_{H_2}}{K^{I}_{H_2}} = e^{\frac{F}{RT}(E^0 - E^0_{H_2})} = 2.62\times10^{-5}$$

Table S1: Selected geometrical parameters, Mayer's bond orders, and HOMO/LUMO energies (eV), of complexes **1** and **2**.[a]

	1	**2**
Bond Lengths (Å)		
Ni-S1	2.195 (2.165)	2.190 (2.161)
Ni-S2	2.191 (2.161)	2.189 (2.159)
Ni-P1	2.224 (2.208)	2.172 (2.153)
Ni-P2	2.240 (2.221)	2.174 (2.156)
Bond Angles (°)		
S1-Ni-S2	90.5 (90.4)	92.0 (92.2)
P1-Ni-P2	103.1 (103.7)	90.1 (90.5)
Bond Orders		
Ni-S1	0.96(0.96)	0.95(0.89)
Ni-S2	0.97(0.97)	0.96(0.90)
Ni-P1	0.87(0.91)	0.96(0.95)
Ni-P2	0.86(0.85)	0.96(0.94)
HOMO/LUMO Energies (eV)		
HOMO	-4.4	-4.4
LUMO	-1.4	-1.3

[a]The numbers outside the parentheses have been obtained at the B3LYP/6-31G* level of theory and those within, have been obtained at the BP86 (ZORA)/def2-TZVP level of theory.

Table S2: Selected geometrical parameters, and Mayer's bond orders of various structures shown in Figure 6.[a]

	1	**20**	**31**	**32**	**41**	**42**	**TS**	**50**
Bond Lengths (Å)								
Ni-S1	2.195 (2.165)	2.304	2.208 (2.188)	2.450 (2.237)	2.291 (2.238)	2.263 (2.219)	2.240	2.200
Ni-S2	2.191 (2.161)	2.303	2.235 (2.202)	2.254 (2.199)	2.283 (2.235)	2.386 (2.277)	2.286	2.206
Ni-P1	2.224 (2.208)	2.203	2.335 (2.272)	2.224 (2.211)	2.222 (2.214)	2.092 (2.138)	2.235	2.204
Ni-P2	2.240 (2.221)	2.203	2.242 (2.199)	2.242 (2.220)	2.190 (2.195)	2.091 (2.132)	2.443	2.203
Ni-Fe	4.294 (4.288)	4.255	4.225 (4.200)	4.212 (4.232)	4.131 (4.176)	4.131 (4.184)	4.339	4.253
Ni-H			1.468 (1.472)		1.470 (1.472)		1.464/ 1.441	
S-H				1.352 (1.364)		1.363 (1.372)		
H-H							1.286	0.745
Bond Angles (°)								
S1-Ni-S2	90.5 (90.4)	91.5	92.3 (91.9)	89.6 (90.3)	90.4 (91.0)	89.2 (91.9)	90.4	91.5
P1-Ni-P2	103.1 (103.7)	105.9	106.4 (107.6)	105.9 (106.6)	112.0 (109.0)	112.4 (110.8)	101.1	106.1
Td dihedral (°)[b]								
	32.1 (32.0)	66.8	75.7 (78.4)	81.1 (73.7)	88.0 (91.9)	86.5 (90.5)	73.7	45.8
Bond Orders								
Ni-S1	0.96(0.96)	0.76	1.08(1.00)	0.39(0.73)	0.81(0.85)	0.59(0.70)	0.95	0.91
Ni-S2	0.97(0.97)	0.76	0.95(0.90)	0.87(0.95)	0.80(0.78)	0.56(0.68)	0.82	0.91
Ni-P1	0.87(0.91)	0.92	0.78(0.74)	0.89(0.93)	0.93(0.88)	1.26(1.08)	0.9	0.88
Ni-P2	0.86(0.85)	0.93	0.84(0.85)	0.83(0.93)	0.96(0.85)	1.21(1.07)	0.64	0.9
Ni-H			0.84(0.79)		0.87 (0.81)		0.80/ 0.75	
S-H				0.90 (0.89)		0.85 (0.89)		

[a]The numbers outside the parentheses have been obtained at the B3LYP/6-31G* level of theory and those within, have been obtained at the BP86 (ZORA)/def2-TZVP level of theory.

[b]The "Td dihedral" is the angle between the normal vectors of the S1-Ni-S2 and P1-Ni-P2 planes.

Table S3: HOMO/LUMO energies (eV), and contributions (%) of different fragments to the corresponding HOMOs and LUMOs.[a]

	HOMO							LUMO						
	1	**20**	**31**	**32**	**41**	**42**	**50**	**1**	**20**	**31**	**32**	**41**	**42**	**50**
α	-4.4	-0.7	-4.3	-4.4	-0.6	-0.6	-4.5	-1.4	1.9	-1.4	-0.7	1.9	2.2	-1.8
β	-4.4	-0.8	-4.8	-4.1	-0.6	-0.6	-4.5	-1.4	1.9	-2.0	-0.9	1.9	2.2	-1.8
Ni(s)	0	0	0	2	0	1	0	0	0	1	0	0	0	0
Ni(p)	5	1	1	6	0	8	5	3	0	3	8	0	0	5
Ni(d)	9	14	7	57	26	48	12	41	1	53	35	1	1	38
d_{z^2}	0	0	0	4	0	2	0	0	0	2	1	0	0	0
d_{xz}	1	1	0	44	2	2	2	1	0	2	0	0	0	0
d_{yz}	8	0	0	7	0	0	10	1	0	7	3	0	0	1
$d_{x^2-y^2}$	0	1	5	1	1	2	0	28	0	31	30	0	0	22
d_{xy}	0	12	1	0	22	42	0	11	1	11	0	0	0	15
Fe(s)	0	0	0	0	0	0	0	0	0	0	0	0	0	0
Fe(p)	0	0	0	0	0	0	0	0	0	0	0	0	0	0
Fe(d)	0	1	1	0	1	1	0	2	1	1	1	1	1	2
S1(s)	0	0	0	0	0	0	0	0	0	0	0	0	0	0
S1(p)	19	25	25	5	26	1	20	12	0	11	1	0	0	11
S1(d)	0	0	0	0	0	0	0	0	0	0	0	0	0	0
S2(s)	0	0	0	0	0	0	0	0	0	0	0	0	0	0
S2(p)	24	25	24	15	17	15	25	12	0	7	3	0	0	11
S2(d)	0	0	0	0	0	0	0	0	0	0	0	0	0	0
P1(s)	0	1	1	-1	1	-1	0	1	0	1	0	0	0	1
P1(p)	2	3	4	4	3	5	2	4	2	5	5	0	0	5
P1(d)	0	0	0	1	0	1	0	1	1	0	1	0	0	1
P2(s)	0	1	0	0	1	0	0	1	0	0	-1	0	0	1
P2(p)	2	3	2	1	2	4	2	4	0	2	4	5	4	6
P2(d)	0	0	0	0	0	0	0	1	1	0	1	2	2	1
phenyl	34	20	31	4	17	6	30	3	0	5	7	0	0	3
cyclo	0	2	1	0	1	1	0	3	4	2	2	4	3	3
rings	3	4	3	3	5	9	3	11	87	7	31	87	90	13
H/H2			0	0	0	2	0			0	2	0	0	0

Since these are open-shell calculations, the HOMO, LUMOs (highlighted in red) are based on the relative energies of the corresponding α and β orbitals.

Table S3 (contd.): HOMO/LUMO energies (eV), and contributions (%) of different fragments to the corresponding HOMOs and LUMOs.

	HOMO							**LUMO**						
	1	**20**	**31**	**32**	**41**	**42**	**50**	**1**	**20**	**31**	**32**	**41**	**42**	**50**
phenyl(s)	0	0	0	0	0	0	0	0	0	0	0	0	0	0
phenyl(p)	34	19	30	3	17	6	29	2	0	5	7	0	0	3
phenyl(d)	1	1	1	0	0	0	1	0	0	0	0	0	0	0
cyclo(s)	0	0	0	0	0	0	0	0	1	0	1	1	1	1
cyclo(p)	0	1	1	0	1	1	0	3	2	2	1	3	2	3
cyclo(d)	0	0	0	0	0	0	0	0	0	0	0	0	0	0
rings(s)	1	0	1	1	1	1	1	1	1	0	1	1	1	0
rings(p)	2	3	2	3	4	7	2	9	84	7	29	84	87	12
rings(d)	0	0	0	0	0	0	0	0	2	0	1	2	2	0

Table S4. X-ray crystallographic data collection and refinement statistics.

Crystal Data

Moiety Formula	2(C40 H32 Fe Ni P2 S2), 0.5(C6 H14), C4 H10 O
Stoichiometric Formula	C87 H81 Fe2 Ni2 O P4 S4
Formula Weight M_r	1623.76
Cell Setting	monoclinic
Space Group (H-M)	P 1 21/c 1
Space Group (Hall)	-P 2ybc
Crystal Description	plate
Crystal Color	clear dark brown
Crystal Size Max (mm)	0.230
Crystal Size Mid (mm)	0.100
Crystal Size Min (mm)	0.030
D_x (Mg m^{-3})	1.453
Density Method	not measured
F(000)	3372
Absorption Coefficient μ (mm^{-1})	1.130
a	21.617(4)
b	20.506(4)
c	17.509(3)
α	90
β	106.928(3)
γ	90
V	7425.(2)
Z	4
Cell Measurement Temperature (°K)	123.(2)
Reflections Used for Cell Parameters	3052
Cell Measurement θ_{min}	2.2059
Cell Measurement θ_{max}	20.5343

Data Collection

Data Collection Temperature (°K)	123.(2)
Data Collection Wavelength (Å)	0.71073
Radiation Type	MoKα
Radiation Source	Fine focus sealed tube
Radiation Monochromator Type	graphite
Measurement Device	Bruker Smart APEX
Measurement Method	ω and ϕ scans
Area Detector Mean Resolution	8.3330
Number of Measured Reflections	59535
R_{int}	0.1034
[Σ|σ(I)|]/[|net(I)|]	0.0830

h_{min}	-25
h_{max}	25
k_{min}	-24
k_{max}	24
l_{min}	-20
l_{max}	20
θ_{min}	1.65
θ_{max}	25.09
Number of Independent Reflections	13157
Number of Observed Reflections	8954
Observed Criterion	>2sigma(I)
Absorption Correction Type	multi-scan
Absorption Correction Details	SADABS Version 2008/1 (Bruker AXS, 2008)
Minimum Transmission T_{min}	0.85
Maximum Transmission T_{max}	0.97
Coverage Fraction$_{max}$	0.996
θ_{full}	25.09
Coverage Fraction$_{full}$	0.996

Refinement

Structure Factors for Least-Squares	Fsqd
Least-Squares Derivatives Matrix	full
Weighting Scheme for Least-Squares	calc

Weighting Scheme Details

calc $w=1/[\sigma^2(Fo^2)+(0.0340P)^2+4.3369P]$ where $P=(Fo^2+2Fc^2)/3$

Primary Structure Solution	direct
Secondary Structure Solution	difmap
Hydrogen Sites Solution	geom
Hydrogen Sites Refinement	constr
Extinction Correction Method	none
Reflections Used in L.S. Derivatives	13157
Parameters Refined	901
Number of Restraints	3
R_{all}	0.0857
R_{obs}	0.0472
wR_{all}	0.1046
wR_{obs}	0.0896
Goodness of Fit (S)	1.002
Restrained Goodness of Fit	1.002
$(\Delta/\sigma)_{max}$	0.001
$(\Delta/\sigma)_{mean}$	0.000
Max $e^-/Å^3$ in final diff. map	0.852

Min $e^-/Å^3$ in final diff. map -0.767

Special Details on the Refinement
Refinement of F^2 against ALL reflections. The weighted R-factor wR and goodness of fit S are based on F^2, conventional R-factors R are based on F, with F set to zero for negative F^2. The threshold expression of F^2> 2sigma(F^2) is used only for calculating R-factors(gt) etc. and is not relevant to the choice of reflections for refinement. R-factors based on F^2 are statistically about twice as large as those based on F, and R- factors based on ALL data will be even larger.

Additional Geometrical Details
All esds (except the esd in the dihedral angle between two l.s. planes) are estimated using the full covariance matrix. The cell esds are taken into account individually in the estimation of esds in distances, angles and torsion angles; correlations between esds in cell parameters are only used when they are defined by crystal symmetry. An approximate (isotropic) treatment of cell esds is used for estimating esds involving l.s. planes.

Software

Data Collection Bruker Instrument Service v2010, 9, 0, 0 (Bruker AXS, 2010)
Cell Refinement SAINT V7.68A (Bruker AXS, 2009)
Data Reduction SAINT V7.68A (Bruker AXS, 2009)
Structure Solution SHELXS-97 (Sheldrick, 2008)
Structure Refinement SHELXL-97 (Sheldrick, 2008)
Molecular Graphics XShell ver. 6.3.1 (Bruker AXS, 2004)
Publication Material Bruker APEX2 v2010.9-1 (Bruker AXS, 2010)

Table S5. Crystallographically determined bond lengths for **1.**

Atom 1	Atom 2	Distance
Ni1A	S2A	2.1657(12)
Ni1A	S1A	2.1661(12)
Ni1A	P1A	2.2228(12)
Ni1A	P2A	2.2264(12)
Fe1A	C7A	2.011(4)
Fe1A	C12A	2.013(4)
Fe1A	C13A	2.021(4)
Fe1A	C8A	2.028(4)
Fe1A	C11A	2.031(4)
Fe1A	C16A	2.045(4)
Fe1A	C14A	2.049(4)
Fe1A	C10A	2.055(4)
Fe1A	C9A	2.059(4)
Fe1A	C15A	2.061(4)
S1A	C1A	1.747(4)
S2A	C2A	1.752(4)
P1A	C7A	1.808(4)
P1A	C17A	1.823(4)
P1A	C23A	1.843(4)
P2A	C12A	1.813(4)
P2A	C35A	1.822(4)
P2A	C29A	1.841(4)
C1A	C6A	1.400(5)
C1A	C2A	1.402(6)
C2A	C3A	1.395(6)
C3A	C4A	1.381(6)
C3A	H3A	0.95
C4A	C5A	1.390(6)
C4A	H4A	0.95
C5A	C6A	1.382(6)
C5A	H5A	0.95
C6A	H6A	0.95
C7A	C8A	1.436(5)
C7A	C11A	1.437(6)
C8A	C9A	1.416(6)
C8A	H8A	0.95
C9A	C10A	1.411(6)
C9A	H9A	0.95
C10A	C11A	1.414(6)
C10A	H10A	0.95
C11A	H11A	0.95
C12A	C13A	1.435(5)

C12A	C16A	1.442(5)
C13A	C14A	1.417(6)
C13A	H13A	0.95
C14A	C15A	1.404(6)
C14A	H14A	0.95
C15A	C16A	1.421(5)
C15A	H15A	0.95
C16A	H16A	0.95
C17A	C22A	1.391(6)
C17A	C18A	1.404(6)
C18A	C19A	1.385(6)
C18A	H18A	0.95
C19A	C20A	1.387(7)
C19A	H19A	0.95
C20A	C21A	1.371(7)
C20A	H20A	0.95
C21A	C22A	1.391(6)
C21A	H21A	0.95
C22A	H22A	0.95
C23A	C28A	1.386(6)
C23A	C24A	1.386(6)
C24A	C25A	1.383(6)
C24A	H24A	0.95
C25A	C26A	1.372(6)
C25A	H25A	0.95
C26A	C27A	1.382(6)
C26A	H26A	0.95
C27A	C28A	1.382(6)
C27A	H27A	0.95
C28A	H28A	0.95
C29A	C34A	1.387(6)
C29A	C30A	1.396(6)
C30A	C31A	1.392(6)
C30A	H30A	0.95
C31A	C32A	1.376(6)
C31A	H31A	0.95
C32A	C33A	1.374(6)
C32A	H32A	0.95
C33A	C34A	1.394(6)
C33A	H33A	0.95
C34A	H34A	0.95
C35A	C36A	1.388(5)
C35A	C40A	1.395(5)
C36A	C37A	1.383(6)
C36A	H36A	0.95
C37A	C38A	1.381(6)

C37A	H37A	0.95
C38A	C39A	1.382(6)
C38A	H38A	0.95
C39A	C40A	1.382(6)
C39A	H39A	0.95
C40A	H40A	0.95
Ni1B	S1B	2.1647(12)
Ni1B	S2B	2.1788(12)
Ni1B	P2B	2.2175(12)
Ni1B	P1B	2.2462(12)
Fe1B	C12B	2.002(4)
Fe1B	C7B	2.013(4)
Fe1B	C13B	2.014(4)
Fe1B	C11B	2.017(4)
Fe1B	C16B	2.037(4)
Fe1B	C8B	2.038(4)
Fe1B	C10B	2.050(4)
Fe1B	C9B	2.053(4)
Fe1B	C14B	2.053(4)
Fe1B	C15B	2.059(4)
P1B	C7B	1.829(4)
P1B	C17B	1.831(4)
P1B	C23B	1.835(4)
P2B	C12B	1.806(4)
P2B	C35B	1.826(4)
P2B	C29B	1.831(4)
S1B	C1B	1.752(4)
S2B	C2B	1.756(4)
C1B	C2B	1.398(6)
C1B	C6B	1.401(5)
C2B	C3B	1.393(6)
C3B	C4B	1.391(6)
C3B	H3B	0.95
C4B	C5B	1.383(6)
C4B	H4B	0.95
C5B	C6B	1.376(6)
C5B	H5B	0.95
C6B	H6B	0.95
C7B	C8B	1.428(6)
C7B	C11B	1.435(6)
C8B	C9B	1.419(6)
C8B	H8B	0.95
C9B	C10B	1.412(6)
C9B	H9B	0.95
C10B	C11B	1.415(6)
C10B	H10B	0.95

C11B	H11B	0.95
C12B	C16B	1.428(5)
C12B	C13B	1.444(6)
C13B	C14B	1.414(6)
C13B	H13B	0.95
C14B	C15B	1.422(6)
C14B	H14B	0.95
C15B	C16B	1.421(6)
C15B	H15B	0.95
C16B	H16B	0.95
C17B	C22B	1.373(6)
C17B	C18B	1.394(6)
C18B	C19B	1.390(7)
C18B	H18B	0.95
C19B	C20B	1.352(9)
C19B	H19B	0.95
C20B	C21B	1.394(8)
C20B	H20B	0.95
C21B	C22B	1.392(7)
C21B	H21B	0.95
C22B	H22B	0.95
C23B	C28B	1.374(6)
C23B	C24B	1.383(6)
C24B	C25B	1.389(6)
C24B	H24B	0.95
C25B	C26B	1.368(6)
C25B	H25B	0.95
C26B	C27B	1.378(8)
C26B	H26B	0.95
C27B	C28B	1.377(7)
C27B	H27B	0.95
C28B	H28B	0.95
C29B	C34B	1.387(5)
C29B	C30B	1.399(6)
C30B	C31B	1.390(6)
C30B	H30B	0.95
C31B	C32B	1.380(6)
C31B	H31B	0.95
C32B	C33B	1.380(6)
C32B	H32B	0.95
C33B	C34B	1.389(6)
C33B	H33B	0.95
C34B	H34B	0.95
C35B	C40B	1.394(6)
C35B	C36B	1.395(6)
C36B	C37B	1.384(6)

C36B	H36B	0.95
C37B	C38B	1.371(6)
C37B	H37B	0.95
C38B	C39B	1.388(7)
C38B	H38B	0.95
C39B	C40B	1.387(6)
C39B	H39B	0.95
C40B	H40B	0.95
C41	C42	1.524(9)
C41	H41A	0.98
C41	H41B	0.98
C41	H41C	0.98
C42	O43	1.393(6)
C42	H42A	0.99
C42	H42B	0.99
O43	C44	1.456(7)
C44	C45	1.479(8)
C44	H44A	0.99
C44	H44B	0.99
C45	H45A	0.98
C45	H45B	0.98
C45	H45C	0.98
C51	C51^{3}	1.298(7)
C51	C52	1.299(7)
C51	H51A	0.99
C51	H51B	0.99
C52	C53	1.299(7)
C52	H52A	0.99
C52	H52B	0.99
C53	H53A	0.98
C53	H53B	0.98
C53	H53C	0.98

Table S6: Crystallographically determined bond angles for complex 1.

Atom 1	Atom 2	Atom 3	Angle
S2A	Ni1A	S1A	90.66(4)
S2A	Ni1A	P1A	86.12(4)
S1A	Ni1A	P1A	163.07(5)
S2A	Ni1A	P2A	165.47(5)
S1A	Ni1A	P2A	85.55(4)
P1A	Ni1A	P2A	101.43(4)
C7A	Fe1A	C12A	108.70(16)
C7A	Fe1A	C13A	108.35(17)
C12A	Fe1A	C13A	41.66(16)
C7A	Fe1A	C8A	41.64(15)
C12A	Fe1A	C8A	138.07(16)
C13A	Fe1A	C8A	109.64(17)
C7A	Fe1A	C11A	41.64(16)
C12A	Fe1A	C11A	110.27(16)
C13A	Fe1A	C11A	138.10(17)
C8A	Fe1A	C11A	69.01(17)
C7A	Fe1A	C16A	139.42(16)
C12A	Fe1A	C16A	41.62(15)
C13A	Fe1A	C16A	69.19(16)
C8A	Fe1A	C16A	178.49(17)
C11A	Fe1A	C16A	112.50(17)
C7A	Fe1A	C14A	137.13(17)
C12A	Fe1A	C14A	69.29(16)
C13A	Fe1A	C14A	40.76(16)
C8A	Fe1A	C14A	110.40(17)
C11A	Fe1A	C14A	178.65(17)
C16A	Fe1A	C14A	68.09(17)
C7A	Fe1A	C10A	69.38(17)
C12A	Fe1A	C10A	139.27(17)
C13A	Fe1A	C10A	177.63(17)
C8A	Fe1A	C10A	68.26(17)
C11A	Fe1A	C10A	40.49(16)
C16A	Fe1A	C10A	112.92(17)
C14A	Fe1A	C10A	140.61(17)
C7A	Fe1A	C9A	69.30(16)
C12A	Fe1A	C9A	177.98(16)
C13A	Fe1A	C9A	138.83(17)
C8A	Fe1A	C9A	40.52(16)
C11A	Fe1A	C9A	68.10(17)
C16A	Fe1A	C9A	139.85(17)
C14A	Fe1A	C9A	112.31(17)
C10A	Fe1A	C9A	40.12(16)

C7A	Fe1A	C15A	176.67(17)
C12A	Fe1A	C15A	69.26(16)
C13A	Fe1A	C15A	68.35(17)
C8A	Fe1A	C15A	138.35(16)
C11A	Fe1A	C15A	141.25(17)
C16A	Fe1A	C15A	40.50(15)
C14A	Fe1A	C15A	39.95(16)
C10A	Fe1A	C15A	113.91(17)
C9A	Fe1A	C15A	112.76(17)
C1A	S1A	Ni1A	105.92(14)
C2A	S2A	Ni1A	106.06(14)
C7A	P1A	C17A	105.64(19)
C7A	P1A	C23A	100.43(18)
C17A	P1A	C23A	104.86(19)
C7A	P1A	Ni1A	120.75(13)
C17A	P1A	Ni1A	106.28(14)
C23A	P1A	Ni1A	117.41(13)
C12A	P2A	C35A	102.32(18)
C12A	P2A	C29A	100.56(18)
C35A	P2A	C29A	104.35(19)
C12A	P2A	Ni1A	122.05(13)
C35A	P2A	Ni1A	107.84(13)
C29A	P2A	Ni1A	117.53(13)
C6A	C1A	C2A	119.4(4)
C6A	C1A	S1A	121.5(3)
C2A	C1A	S1A	119.0(3)
C3A	C2A	C1A	119.5(4)
C3A	C2A	S2A	122.1(3)
C1A	C2A	S2A	118.3(3)
C4A	C3A	C2A	120.4(4)
C4A	C3A	H3A	119.8
C2A	C3A	H3A	119.8
C3A	C4A	C5A	120.2(4)
C3A	C4A	H4A	119.9
C5A	C4A	H4A	119.9
C6A	C5A	C4A	120.0(4)
C6A	C5A	H5A	120.0
C4A	C5A	H5A	120.0
C5A	C6A	C1A	120.4(4)
C5A	C6A	H6A	119.8
C1A	C6A	H6A	119.8
C8A	C7A	C11A	106.4(4)
C8A	C7A	P1A	128.8(3)
C11A	C7A	P1A	124.8(3)
C8A	C7A	Fe1A	69.8(2)
C11A	C7A	Fe1A	69.9(2)

P1A	C7A	Fe1A	122.9(2)
C9A	C8A	C7A	108.5(4)
C9A	C8A	Fe1A	70.9(2)
C7A	C8A	Fe1A	68.5(2)
C9A	C8A	H8A	125.7
C7A	C8A	H8A	125.7
Fe1A	C8A	H8A	126.4
C10A	C9A	C8A	108.3(4)
C10A	C9A	Fe1A	69.8(2)
C8A	C9A	Fe1A	68.6(2)
C10A	C9A	H9A	125.9
C8A	C9A	H9A	125.9
Fe1A	C9A	H9A	127.4
C9A	C10A	C11A	108.3(4)
C9A	C10A	Fe1A	70.1(2)
C11A	C10A	Fe1A	68.8(2)
C9A	C10A	H10A	125.8
C11A	C10A	H10A	125.8
Fe1A	C10A	H10A	126.8
C10A	C11A	C7A	108.5(4)
C10A	C11A	Fe1A	70.7(2)
C7A	C11A	Fe1A	68.4(2)
C10A	C11A	H11A	125.7
C7A	C11A	H11A	125.7
Fe1A	C11A	H11A	126.7
C13A	C12A	C16A	106.7(3)
C13A	C12A	P2A	126.9(3)
C16A	C12A	P2A	126.4(3)
C13A	C12A	Fe1A	69.4(2)
C16A	C12A	Fe1A	70.4(2)
P2A	C12A	Fe1A	123.8(2)
C14A	C13A	C12A	108.1(4)
C14A	C13A	Fe1A	70.7(2)
C12A	C13A	Fe1A	68.9(2)
C14A	C13A	H13A	125.9
C12A	C13A	H13A	125.9
Fe1A	C13A	H13A	126.1
C15A	C14A	C13A	108.7(4)
C15A	C14A	Fe1A	70.5(2)
C13A	C14A	Fe1A	68.6(2)
C15A	C14A	H14A	125.6
C13A	C14A	H14A	125.6
Fe1A	C14A	H14A	126.9
C14A	C15A	C16A	108.4(4)
C14A	C15A	Fe1A	69.6(2)
C16A	C15A	Fe1A	69.2(2)

C14A	C15A	H15A	125.8
C16A	C15A	H15A	125.8
Fe1A	C15A	H15A	127.1
C15A	C16A	C12A	107.9(4)
C15A	C16A	Fe1A	70.3(2)
C12A	C16A	Fe1A	68.0(2)
C15A	C16A	H16A	126.0
C12A	C16A	H16A	126.0
Fe1A	C16A	H16A	127.2
C22A	C17A	C18A	118.6(4)
C22A	C17A	P1A	117.7(3)
C18A	C17A	P1A	123.7(3)
C19A	C18A	C17A	120.5(5)
C19A	C18A	H18A	119.8
C17A	C18A	H18A	119.8
C18A	C19A	C20A	120.2(5)
C18A	C19A	H19A	119.9
C20A	C19A	H19A	119.9
C21A	C20A	C19A	119.7(5)
C21A	C20A	H20A	120.2
C19A	C20A	H20A	120.2
C20A	C21A	C22A	120.9(5)
C20A	C21A	H21A	119.5
C22A	C21A	H21A	119.5
C21A	C22A	C17A	120.1(4)
C21A	C22A	H22A	119.9
C17A	C22A	H22A	119.9
C28A	C23A	C24A	119.0(4)
C28A	C23A	P1A	117.3(3)
C24A	C23A	P1A	123.7(3)
C25A	C24A	C23A	120.0(4)
C25A	C24A	H24A	120.0
C23A	C24A	H24A	120.0
C26A	C25A	C24A	120.9(4)
C26A	C25A	H25A	119.5
C24A	C25A	H25A	119.5
C25A	C26A	C27A	119.3(4)
C25A	C26A	H26A	120.4
C27A	C26A	H26A	120.4
C26A	C27A	C28A	120.3(4)
C26A	C27A	H27A	119.9
C28A	C27A	H27A	119.9
C27A	C28A	C23A	120.5(4)
C27A	C28A	H28A	119.7
C23A	C28A	H28A	119.7
C34A	C29A	C30A	118.8(4)

C34A	C29A	P2A	119.2(3)
C30A	C29A	P2A	122.0(3)
C31A	C30A	C29A	119.7(4)
C31A	C30A	H30A	120.2
C29A	C30A	H30A	120.2
C32A	C31A	C30A	120.6(4)
C32A	C31A	H31A	119.7
C30A	C31A	H31A	119.7
C33A	C32A	C31A	120.4(4)
C33A	C32A	H32A	119.8
C31A	C32A	H32A	119.8
C32A	C33A	C34A	119.4(4)
C32A	C33A	H33A	120.3
C34A	C33A	H33A	120.3
C29A	C34A	C33A	121.1(4)
C29A	C34A	H34A	119.4
C33A	C34A	H34A	119.4
C36A	C35A	C40A	118.0(4)
C36A	C35A	P2A	119.9(3)
C40A	C35A	P2A	121.9(3)
C37A	C36A	C35A	120.9(4)
C37A	C36A	H36A	119.6
C35A	C36A	H36A	119.6
C38A	C37A	C36A	120.4(4)
C38A	C37A	H37A	119.8
C36A	C37A	H37A	119.8
C37A	C38A	C39A	119.6(4)
C37A	C38A	H38A	120.2
C39A	C38A	H38A	120.2
C38A	C39A	C40A	119.9(4)
C38A	C39A	H39A	120.1
C40A	C39A	H39A	120.1
C39A	C40A	C35A	121.2(4)
C39A	C40A	H40A	119.4
C35A	C40A	H40A	119.4
S1B	Ni1B	S2B	90.24(4)
S1B	Ni1B	P2B	84.89(4)
S2B	Ni1B	P2B	174.87(5)
S1B	Ni1B	P1B	174.04(5)
S2B	Ni1B	P1B	85.52(4)
P2B	Ni1B	P1B	99.21(5)
C12B	Fe1B	C7B	107.95(16)
C12B	Fe1B	C13B	42.15(16)
C7B	Fe1B	C13B	110.80(17)
C12B	Fe1B	C11B	109.99(17)
C7B	Fe1B	C11B	41.73(17)

C13B	Fe1B	C11B	140.72(17)
C12B	Fe1B	C16B	41.40(16)
C7B	Fe1B	C16B	135.91(17)
C13B	Fe1B	C16B	69.58(17)
C11B	Fe1B	C16B	109.10(18)
C12B	Fe1B	C8B	136.60(17)
C7B	Fe1B	C8B	41.26(16)
C13B	Fe1B	C8B	110.23(17)
C11B	Fe1B	C8B	69.11(18)
C16B	Fe1B	C8B	177.10(16)
C12B	Fe1B	C10B	140.16(18)
C7B	Fe1B	C10B	69.21(17)
C13B	Fe1B	C10B	177.68(18)
C11B	Fe1B	C10B	40.71(16)
C16B	Fe1B	C10B	112.12(18)
C8B	Fe1B	C10B	68.15(18)
C12B	Fe1B	C9B	177.01(17)
C7B	Fe1B	C9B	69.19(17)
C13B	Fe1B	C9B	137.45(17)
C11B	Fe1B	C9B	68.61(17)
C16B	Fe1B	C9B	141.36(17)
C8B	Fe1B	C9B	40.57(16)
C10B	Fe1B	C9B	40.25(17)
C12B	Fe1B	C14B	69.54(17)
C7B	Fe1B	C14B	141.18(18)
C13B	Fe1B	C14B	40.68(16)
C11B	Fe1B	C14B	177.08(18)
C16B	Fe1B	C14B	68.56(17)
C8B	Fe1B	C14B	113.31(18)
C10B	Fe1B	C14B	138.02(17)
C9B	Fe1B	C14B	112.00(17)
C12B	Fe1B	C15B	69.26(17)
C7B	Fe1B	C15B	176.50(17)
C13B	Fe1B	C15B	68.73(17)
C11B	Fe1B	C15B	136.61(18)
C16B	Fe1B	C15B	40.59(16)
C8B	Fe1B	C15B	142.23(17)
C10B	Fe1B	C15B	111.41(18)
C9B	Fe1B	C15B	113.62(17)
C14B	Fe1B	C15B	40.47(17)
C7B	P1B	C17B	101.4(2)
C7B	P1B	C23B	99.79(19)
C17B	P1B	C23B	104.6(2)
C7B	P1B	Ni1B	123.11(14)
C17B	P1B	Ni1B	111.15(15)
C23B	P1B	Ni1B	114.58(15)

C12B	P2B	C35B	106.71(19)
C12B	P2B	C29B	99.43(18)
C35B	P2B	C29B	104.74(19)
C12B	P2B	Ni1B	115.83(14)
C35B	P2B	Ni1B	110.01(14)
C29B	P2B	Ni1B	118.82(13)
C1B	S1B	Ni1B	105.85(14)
C2B	S2B	Ni1B	105.76(14)
C2B	C1B	C6B	119.8(4)
C2B	C1B	S1B	119.3(3)
C6B	C1B	S1B	120.9(3)
C3B	C2B	C1B	119.6(4)
C3B	C2B	S2B	122.6(3)
C1B	C2B	S2B	117.8(3)
C4B	C3B	C2B	119.7(4)
C4B	C3B	H3B	120.2
C2B	C3B	H3B	120.2
C5B	C4B	C3B	120.7(4)
C5B	C4B	H4B	119.7
C3B	C4B	H4B	119.7
C6B	C5B	C4B	120.1(4)
C6B	C5B	H5B	119.9
C4B	C5B	H5B	119.9
C5B	C6B	C1B	120.0(4)
C5B	C6B	H6B	120.0
C1B	C6B	H6B	120.0
C8B	C7B	C11B	106.9(4)
C8B	C7B	P1B	127.3(3)
C11B	C7B	P1B	125.8(3)
C8B	C7B	Fe1B	70.3(2)
C11B	C7B	Fe1B	69.3(2)
P1B	C7B	Fe1B	125.6(2)
C9B	C8B	C7B	108.4(4)
C9B	C8B	Fe1B	70.3(2)
C7B	C8B	Fe1B	68.4(2)
C9B	C8B	H8B	125.8
C7B	C8B	H8B	125.8
Fe1B	C8B	H8B	127.1
C10B	C9B	C8B	108.1(4)
C10B	C9B	Fe1B	69.8(2)
C8B	C9B	Fe1B	69.2(2)
C10B	C9B	H9B	126.0
C8B	C9B	H9B	126.0
Fe1B	C9B	H9B	126.7
C9B	C10B	C11B	108.5(4)
C9B	C10B	Fe1B	70.0(2)

C11B	C10B	Fe1B	68.4(2)
C9B	C10B	H10B	125.8
C11B	C10B	H10B	125.8
Fe1B	C10B	H10B	127.5
C10B	C11B	C7B	108.1(4)
C10B	C11B	Fe1B	70.9(2)
C7B	C11B	Fe1B	69.0(2)
C10B	C11B	H11B	125.9
C7B	C11B	H11B	125.9
Fe1B	C11B	H11B	125.7
C16B	C12B	C13B	107.2(4)
C16B	C12B	P2B	129.3(3)
C13B	C12B	P2B	123.5(3)
C16B	C12B	Fe1B	70.6(2)
C13B	C12B	Fe1B	69.4(2)
P2B	C12B	Fe1B	124.8(2)
C14B	C13B	C12B	108.0(4)
C14B	C13B	Fe1B	71.2(2)
C12B	C13B	Fe1B	68.5(2)
C14B	C13B	H13B	126.0
C12B	C13B	H13B	126.0
Fe1B	C13B	H13B	126.0
C13B	C14B	C15B	108.3(4)
C13B	C14B	Fe1B	68.2(2)
C15B	C14B	Fe1B	70.0(2)
C13B	C14B	H14B	125.8
C15B	C14B	H14B	125.8
Fe1B	C14B	H14B	127.6
C16B	C15B	C14B	108.2(4)
C16B	C15B	Fe1B	68.9(2)
C14B	C15B	Fe1B	69.5(2)
C16B	C15B	H15B	125.9
C14B	C15B	H15B	125.9
Fe1B	C15B	H15B	127.3
C15B	C16B	C12B	108.2(4)
C15B	C16B	Fe1B	70.6(2)
C12B	C16B	Fe1B	68.0(2)
C15B	C16B	H16B	125.9
C12B	C16B	H16B	125.9
Fe1B	C16B	H16B	127.1
C22B	C17B	C18B	118.3(5)
C22B	C17B	P1B	119.2(4)
C18B	C17B	P1B	122.4(4)
C19B	C18B	C17B	119.7(6)
C19B	C18B	H18B	120.1
C17B	C18B	H18B	120.1

C20B	C19B	C18B	121.5(6)
C20B	C19B	H19B	119.3
C18B	C19B	H19B	119.3
C19B	C20B	C21B	119.8(5)
C19B	C20B	H20B	120.1
C21B	C20B	H20B	120.1
C22B	C21B	C20B	118.7(6)
C22B	C21B	H21B	120.6
C20B	C21B	H21B	120.6
C17B	C22B	C21B	121.9(5)
C17B	C22B	H22B	119.0
C21B	C22B	H22B	119.0
C28B	C23B	C24B	117.8(4)
C28B	C23B	P1B	120.3(4)
C24B	C23B	P1B	121.9(3)
C23B	C24B	C25B	121.3(4)
C23B	C24B	H24B	119.4
C25B	C24B	H24B	119.4
C26B	C25B	C24B	119.8(4)
C26B	C25B	H25B	120.1
C24B	C25B	H25B	120.1
C25B	C26B	C27B	119.4(5)
C25B	C26B	H26B	120.3
C27B	C26B	H26B	120.3
C28B	C27B	C26B	120.4(5)
C28B	C27B	H27B	119.8
C26B	C27B	H27B	119.8
C23B	C28B	C27B	121.2(5)
C23B	C28B	H28B	119.4
C27B	C28B	H28B	119.4
C34B	C29B	C30B	118.8(4)
C34B	C29B	P2B	118.4(3)
C30B	C29B	P2B	122.7(3)
C31B	C30B	C29B	119.7(4)
C31B	C30B	H30B	120.2
C29B	C30B	H30B	120.2
C32B	C31B	C30B	120.9(4)
C32B	C31B	H31B	119.6
C30B	C31B	H31B	119.6
C33B	C32B	C31B	119.7(4)
C33B	C32B	H32B	120.1
C31B	C32B	H32B	120.1
C32B	C33B	C34B	119.8(4)
C32B	C33B	H33B	120.1
C34B	C33B	H33B	120.1
C29B	C34B	C33B	121.0(4)

C29B	C34B	H34B	119.5
C33B	C34B	H34B	119.5
C40B	C35B	C36B	118.8(4)
C40B	C35B	P2B	123.4(3)
C36B	C35B	P2B	117.8(3)
C37B	C36B	C35B	120.5(4)
C37B	C36B	H36B	119.7
C35B	C36B	H36B	119.7
C38B	C37B	C36B	120.2(4)
C38B	C37B	H37B	119.9
C36B	C37B	H37B	119.9
C37B	C38B	C39B	120.3(4)
C37B	C38B	H38B	119.9
C39B	C38B	H38B	119.9
C40B	C39B	C38B	119.9(4)
C40B	C39B	H39B	120.1
C38B	C39B	H39B	120.1
C39B	C40B	C35B	120.3(4)
C39B	C40B	H40B	119.9
C35B	C40B	H40B	119.9
C42	C41	H41A	109.5
C42	C41	H41B	109.5
H41A	C41	H41B	109.5
C42	C41	H41C	109.5
H41A	C41	H41C	109.5
H41B	C41	H41C	109.5
O43	C42	C41	108.6(5)
O43	C42	H42A	110.0
C41	C42	H42A	110.0
O43	C42	H42B	110.0
C41	C42	H42B	110.0
H42A	C42	H42B	108.4
C42	O43	C44	113.2(5)
O43	C44	C45	108.8(5)
O43	C44	H44A	109.9
C45	C44	H44A	109.9
O43	C44	H44B	109.9
C45	C44	H44B	109.9
H44A	C44	H44B	108.3
C44	C45	H45A	109.5
C44	C45	H45B	109.5
H45A	C45	H45B	109.5
C44	C45	H45C	109.5
H45A	C45	H45C	109.5
H45B	C45	H45C	109.5
C51[3]	C51	C52	117.7(9)

C51[3]	C51	H51A	107.9
C52	C51	H51A	107.9
C51[3]	C51	H51B	107.9
C52	C51	H51B	107.9
H51A	C51	H51B	107.2
C53	C52	C51	116.4(11)
C53	C52	H52A	108.2
C51	C52	H52A	108.2
C53	C52	H52B	108.2
C51	C52	H52B	108.2
H52A	C52	H52B	107.3
C52	C53	H53A	109.5
C52	C53	H53B	109.5
H53A	C53	H53B	109.5
C52	C53	H53C	109.5
H53A	C53	H53C	109.5
H53B	C53	H53C	109.5

Complete forms of Abbreviated References:

28. Andreiadis, E. S.; Jacques, P.-A.; Tran, P. D.; Leyris, A.; Chavarot-Kerlidou, M.; Jousselme, B.; Matheron, M.; Pecaut, J.; Palacin, S.; Fontecave, M.; Artero, V. *Nat. Chem.* **2013**, *5*, 48.

69. Frisch, M. J.; Trucks, G. W.; Schlegel, H. B.; Scuseria, G. E.; Robb, M. A.; Cheeseman, J. R.; Montgomery Jr., J. A.; Vreven, T.; Kudin, K. N.; Burant, J. C.; Millam, J. M.; Iyengar, S. S.; Tomasi, J.; Barone, V.; Mennucci, B.; Cossi, M.; Scalmani, G.; Rega, N.; Persson, G. A.; Nakatsuji, H.; Hada, M.; Ehara, M.; Toyota, K.; Fukuda, R.; Hasegawa, J.; Ishida, M.; Niakajima, T.; Honda, Y.; Kitao, O.; Nakai, H.; Klene, M.; Li, X.; Konox, J. E.; Hratchian, H. P.; Cross, J. B.; Bakken, V.; Adamo, C.; Jaramillo, J.; Gomperts, R.; Stratmann, R. E.; Yazyev, O.; Austin, A. J.; Cammi, R.; Pomelli, C.; Ochterski, J. W.; Ayala, P. Y.; Morokuma, K.; Voth, G. A.; Salvador, P.; Dannenberg, J. J.; Zakrzewski, V. G.; Dapprich, S.; Daniels, A. D.; Strain, M. C.; Farkas, O.; Malick, D. K.; Rabuck, A. D.; Raghavachari, K.; Foresman, J. B.; Ortiz, J. V.; Cui, Q.; Baboul, A. G.; Clifford, S.; Cioslowski, J.; Stefanov, B. B.; Liu, G.; Liashenki, A.; Piskorz, P.; Komaromi, I.; Martin, R. L.; Fox, D. J.; Keith, T.; Al-Laham, M. A.; Peng, C. Y.; Nanayakkara, A.; Challacombe, M.; Gill, P. M. W.; Johnson, B.; Chen, W.; Wong, M. W.; Gonzalez, C.; Pople, J. A. *Gaussian 03, Revision C.02*; Gaussian, Inc. : Wallingford, CT, 2004.